Forsman, Nina; Lozhechnikova, Alina; Khakalo, Alexey; Johansson, Leena-Sisko; Vartiainen, Jari; Österberg, Monika

Layer-by-layer assembled hydrophobic coatings for cellulose nanofibril films and textiles, made of polylysine and natural wax particles

Published in:
Carbohydrate Polymers

DOI:
10.1016/j.carbpol.2017.06.007

Published: 01/01/2017

Document Version
Peer-reviewed accepted author manuscript, also known as Final accepted manuscript or Post-print

Please cite the original version:
Forsman, N., Lozhechnikova, A., Khakalo, A., Johansson, L.-S., Vartiainen, J., & Österberg, M. (2017). Layer-by-layer assembled hydrophobic coatings for cellulose nanofibril films and textiles, made of polylysine and natural wax particles. *Carbohydrate Polymers*, *173*, 392-402. https://doi.org/10.1016/j.carbpol.2017.06.007

Layer-by-layer assembled hydrophobic coatings for cellulose nanofibril films and textiles, made of polylysine and natural wax particles.

Nina Forsman,[a,‡] Alina Lozhechnikova,[a,‡] Alexey Khakalo,[a] Leena-Sisko Johansson,[a] Jari Vartiainen[b] and Monika Österberg[a,*]

[a] *Department of Bioproducts and Biosystems, School of Chemical Engineering, Aalto University, P.O. Box 16300, FI-00076 Aalto, Finland*

[b] *VTT Technical Research Centre of Finland Ltd, Biologinkuja 7, P.O. Box 1000, FI-02044 Espoo, Finland*

*Corresponding author: Monika Österberg (monika.osterberg@aalto.fi).

[‡] These authors contributed equally to this work.

Abstract

Herein we present a simple method to render cellulosic materials highly hydrophobic while retaining their breathability and moisture buffering properties, thus allowing for their use as functional textiles. The surfaces are coated via layer-by-layer deposition of two natural components, cationic poly-L-lysine and anionic carnauba wax particles. The combination of multiscale roughness, open film structure, and low surface energy of wax colloids, resulted in long-lasting superhydrophobicity on cotton surface already after two bilayers. Atomic force microscopy, interference microscopy, scanning electron microscopy and X-ray photoelectron spectroscopy were used to decouple structural effects from changes in surface energy. Furthermore, the effect of thermal annealing on the coating was evaluated. The potential of this simple and green approach to enhance the use of natural cellulosic materials is discussed.

Keywords: Layer-by-layer assembly, poly-L-lysine, carnauba wax, textile, cellulose nanofibril films, hydrophobicity

1. Introduction

In line with the principles of Green Chemistry (Jenck, Agterberg, & Droescher, 2004) we should strive to use renewable feedstock and raw materials, design safe chemicals and products and use safe solvents and reactions conditions. Despite these declarations, only 9% of the organic material feedstock in the EU chemical industry was from renewable sources in 2011 (The European Chemical Industry Council, 2014). Out of the renewable materials, cellulose is maybe the most attractive due to its abundance and interesting properties. The use of cellulosic feedstock could be increased in several global industries, for example, in textile and packaging manufacturing. In 2013, 64% of the fibres produced globally were synthetic, while plastic packaging waste in Europe accounted for 15 million tons (CIRFS, 2016; Eurostat, 2016). Therefore, considering the scale of these industries, a small change towards sustainability would have a large impact. However, the hydrophilicity of cellulose makes it sensitive to moisture, thus often limiting its use. Consequently, extensive research has been devoted to increasing the hydrophobicity of cellulosic materials and enhancing their barrier properties in wet or humid conditions.

In the textile field, wearable textiles are often desired to be waterproof but yet breathable at the same time. Most methods to produce such textiles rely on synthetic fibres (Horrocks & Anand,

2015). Commonly used production techniques include tuning the porosity of the material, so that the pores are large enough for water vapor to pass through, but small enough to stop liquid water permeation, or coating the fibres of the textile and leaving the pores uncoated (Mukhopadhyay & Vinay Kumar, 2008).

Biomimetic approaches to textile modification have also been suggested, mainly to achieve superhydrophobic or self-cleaning surfaces due to a combination of nano- and microscale roughness and low surface energy. The roughness has commonly been achieved by applying nanoparticles, like silica (Gao, Zhu, Guo, & Yang, 2009; Xue, Jia, Zhang, & Tian, 2009; Yu, Gu, Meng, & Qing, 2007), ZnO nanorods (Xu & Cai, 2008; Xu, Cai, Wang, & Ge, 2010) and carbon nanotubes (Liu et al., 2007). The low surface energy has been obtained by using different silane compounds (Gao et al., 2009; Xu & Cai, 2008; Xu et al., 2010), some of which also have fluorine in the structure (Xue et al., 2009; Yu et al., 2007). Gao et al. reported negligible changes in air permeability after the coating (Gao et al., 2009), otherwise breathability/moisture buffering properties have not been reported for superhydrophobic substrates.

Another efficient method to introduce hydrophobicity to a fabric is polymer grafting directly onto the surface. Polyethylene glycol (Badanova, Taussarova, & Kutzhanova, 2014), 1,1,2,2-tetrahydroperfluorodecylacrylate (Tsafack & Levalois-Grützmacher, 2007) and 1H,1H,2H,2H-nonafluorohexyl-1-acrylate (Deng et al., 2010), among some others, have been grafted onto cotton to induce hydrophobicity. Badanova et al. reported that the air permeability was unchanged after the grafting reaction (Badanova et al., 2014), but otherwise no results for gas permeability or transfer were reported. Qi et al successfully coated a poly(ethylene terephthalate) substrate with fluorocarbon using ion beam sputtering (Qi et al., 2002). A uniting factor for many of the existing coatings is the use of different fluorine compounds, which provide high hydrophobicity, but come at high cost and are potentially harmful for human health and the environment (Schultz, Barofsky, & Field, 2003). Other conventional chemical methods to increase hydrophobicity in plant fibres (and further on textiles) include acetylation and benozylation (Kalia, Thakur, Celli, Kiechel, & Schauer, 2013). The problem with chemical treatments, however, is that they often require large amounts of hazardous solvents and produce equally hazardous waste (Kalia et al., 2013).

Furthermore, the use of cellulosic feedstock in packaging could be increased through the application of cellulose nanofibril (CNF) films. Recent research advances have shown that CNF films could, due to their dense structure and good barrier properties, have a potential in packaging applications (Lavoine, Desloges, Dufresne, & Bras, 2012). The pure CNF films show good oxygen barrier properties at relative humidity (RH) below 65% (Österberg et al., 2013). To improve their barrier performance at higher RH, several techniques were proposed. Österberg et al. (2013) used a thick paraffin wax coating to hydrophobize the CNF film, while Liu et al. mixed CNF with clay and thus reduced the oxygen transfer rate at 95% RH (Liu et al., 2007). Other methods that proved effective for lowering the oxygen transfer rate include carboxymethylation pre-treatment, acetylation post-treatment or coating of the CNF films onto polymer films (Lavoine et al., 2012). Carboxymethylation and acetylation, as well as natural and synthetic wax coatings, were also found to lower the water vapor transfer rate of the CNF films (Lavoine et al., 2012; Spence, Venditti, Rojas, Pawlak, & Hubbe, 2011).

The layer-by-layer (LbL) deposition is a simple, low-cost, controllable and versatile method for surface modification, and is therefore an attractive alternative to chemical grafting on various

cellulosic substrates, including natural textiles. The method was originally developed to build up polyelectrolyte multilayers, but recently nanoparticles have also been incorporated in the coatings (Cranston & Gray, 2006; Cranston, Gray, & Rutland, 2010; Decher, Hong, & Schmitt, 1992; Dubas, Kumlangdudsana, & Potiyaraj, 2006; Eronen, Laine, Ruokolainen, & Österberg, 2012; Kotov, Dekany, & Fendler, 1995). The possibility to incorporate various particles and charged molecules opened up new opportunities for the development of functional cellulosic materials. The LbL method has been successfully used on cotton fibres to introduce conductivity, fire retardant and antimicrobial properties (Chen et al., 2016; Gomes, Mano, Queiroz, & Gouveia, 2012; Shirvan, Nejad, & Bashari, 2014). The method has also been used to increase the hydrophobicity of the surfaces, by incorporating low surface energy components, such as petroleum based waxes, into the multilayers (Glinel et al., 2004; Gustafsson, Larsson, & Wågberg, 2012). Studies show that the application of carnauba wax dispersions to wood and glass surfaces can greatly increase their hydrophobicity (Bayer et al., 2011; Lozhechnikova, Vahtikari, Hughes, & Österberg, 2015). However, components with opposite charges are required for a successful LbL deposition, while the surfaces of cellulose and carnauba wax particles are both negatively charged. Thus, the poly-L-lysine (PLL) was chosen as a cationic component of the LbL system in this study. PLL is a highly charged polycation from natural resources and it has been previously utilised to introduce antimicrobial properties to silk and wool fibres (Chang, Zhong, & Xu, 2012; Xing et al., 2015).

Superhydrophobic cellulose-based surfaces would be very interesting for both outdoor applications, such as textile roofs, sunscreen textiles, and sports clothing as well as indoor applications, like domestic (Brown & Stevens, 2007). The common line of the current methods for superhydrophobic textile material production is that they mainly rely on synthetic fibres and/or use synthetic polymers as well as various harmful chemicals for surface hydrophobization. In this work, we introduce a simple and green method to hydrophobize cellulosic substrates, by deposing PLL and wax particles onto the surface. The method is fast and easy to perform, while all materials used are renewable and non-toxic. Furthermore, the LbL treatment is completely water-based and thus can be easily transferred to the modern textile production lines (Brown & Stevens, 2007). To get a better understanding of the layer formation and factors affecting it, quartz crystal microbalance with dissipation (QCM-D) was used to study the build-up process on CNF ultrathin films. QCM-D technique has been previously used to study the LbL build-up of poly-L-lysine with hyaluronic acid (Picart et al., 2001) and heparin (Barrantes, Santos, Sotres, & Arnebrant, 2012). However, to the best of authors' knowledge, no multilayer build-up combining PLL and natural wax particles has been previously reported. The applicability of the method to modification of various cellulosic substrates was demonstrated using CNF freestanding films and commercial cotton and linen fabrics.

2. Experimental

2.1. Materials

2.1.1. Poly-L-lysine

0.1 % (w/v) PLL with a molecular weight of 150,000-300,000 was purchased from Sigma-Aldrich. The pH of the PLL was altered using buffer solutions, 0.1 M HCl and 0.1 M NaOH.

2.1.2. Wax dispersion

Refined carnauba wax was purchased from Sigma-Aldrich. The wax dispersion was prepared by adding wax to hot water at 90 °C and sonicating the mixture for 5 min using Ultrasonic Probe Sonifier S-450 with 1/2" extension (Branson Ultrasonics). Right after sonication, the carnauba dispersion was cooled down in an ice bath, and then filtered through a filter funnel with 100-160 µm nominal maximal pore size. More information about the preparation and characterisation of the wax dispersion can be found elsewhere (Lozhechnikova, Bellanger, Michen, Burgert, & Österberg, 2017). For simplicity, the carnauba wax will be further referred to as wax.

2.1.3. Cellulose nanofibrils freestanding films

A never-dried bleached hardwood kraft pulp was used to prepare the CNF dispersion. No chemical or enzymatic pre-treatment was applied, but the pulp was washed into sodium form (Swerin, Odberg, & Lindström, 1990) prior to disintegration in order to control the counterion type and the ionic strength. The pulp was disintegrated using a high-pressure fluidizer (Microfluidics, M-110Y, Microfluidics Int. Co., Newton, MA). The pulp was circulated 6 and 12 passes through the fluidizer to obtain CNF for self-standing films and QCM-D experiments, respectively.

Freestanding CNF films were used as a substrate to study the performance of the coatings. To prepare a film, 100 mL of 0.85% CNF was filtered through a Sefar Nitex polyamine monofilament open mesh fabric with a 10 µm pore size at 2.5 bar pressure. The film was then hot-pressed in a Carver Laboratory press (Fred S. Carver Inc.) for two hours at 100 °C and with a pressure of 1800 kg/cm^2. The prepared films were stored at standard conditions (23 °C and 50% RH). More detailed information about freestanding CNF films and their production can be found elsewhere (Österberg et al., 2013).

2.1.4. Textile samples

Three different natural textiles were purchased from Eurokangas, one 100% linen sample and two 100% cotton samples. Of the cotton samples, one was a lightweight bedsheet fabric, and the other was a thicker fabric. All fabrics were white and were washed with ethanol prior to use. Grammage of the textiles was 138.8 g/m^2 for light cotton, 261.5 g/m^2 for heavy cotton and 236.9 g/m^2 for linen. Grammage values are an average of three measurements.

2.2. Methods

2.2.1. Quartz Crystal Microbalance with Dissipation monitoring

Gold QCM-D crystals were coated with cellulose nanofibrils as described elsewhere (Lozhechnikova et al., 2014) and were then stored in desiccator until used. QCM-D experiments were carried out with the E4 instrument (Q-sense AB, Västra Frölunda, Sweden). Samples were filtered through a 0.45 µm filter prior to use, except for the wax dispersion, which was filtered with a 1 µm filter. All sample solutions were sonicated for five minutes before use, to make them as uniform as possible. The concentration of PLL was 10 mg/L, and of the wax dispersion 100 mg/l.

The adsorption was monitored until a stable plateau in frequency was acquired. The consecutive layer was adsorbed only after a stable plateau was acquired during rinsing. The pumping rate was constantly 0.1 mL/min. Mass changes were calculated according to the Johannsmann equation (Johannsmann, Mathauer, Wegner, & Knoll, 1992), simplified by Naderi (Naderi & Claesson, 2006)(1):

$$\widehat{m}^* = m^0\left(1 + \hat{\jmath}(f)\frac{pf^2d^2}{3}\right) \quad (1)$$

Where $\widehat{m}^*$ is the equivalent mass, m^0 is the true sensed mass, $\hat{\jmath}(f)$ is the complex shear assumed independent of frequency and d is the thickness of the film. The true sensed mass was obtained by plotting the equivalent mass as the function of the square of the resonance frequency.

2.2.2. Zeta potential

The electrophoretic mobility of PLL was measured using Zetasizer Nano-ZS90 (Malvern Instrument Ltd., Worcestershire, U.K.). The zeta (ζ) potential was calculated from the electrophoretic mobility data by the instrument software using the Smoluchowski model.

2.2.3. Coating of CNF freestanding films and fabrics

Layer-by-layer deposition was done on both CNF films and textiles. Prior to the LbL coating, the substrates were soaked in water for a few minutes. Concentrations of the solutions were 10 mg/L for PLL and 10 g/L for wax. The substrates were thoroughly rinsed with water three times in different beakers, to remove non-adsorbed material after adsorption of each layer and only then, the next layer was adsorbed. The immersion time was always five minutes. The samples were dried and stored between blotting sheets in standard conditions, under a light pressure to keep them flat. A few samples were dried at 103 °C for 1 h, and then stored in standard conditions.

2.2.4. Water contact angle (CA)

The water contact angle (CA) was measured with a CAM 2000 (KSV Instruments Ltd, Finland), and the size of the water droplet was 6.5 µL. The static contact angle was measured for 60 seconds, but due to bending of the CNF films when wetted, the contact angle at 5 seconds was used for comparison. For consistency, the contact angle at 5 seconds was also used for QCM-crystals and textiles. At least six parallel samples were tested for each coating.

2.2.5. Atomic Force Microscopy (AFM)

QCM-D crystals and self-standing CNF films were imaged in air using a Nanoscope V MultiMode scanning probe microscope (Bruker Corporation, Massachusetts, USA). Images were recorded in tapping mode. Silicon cantilevers (NSC15/AIBS, MicroMasch, Tallinn, Estonia) with driving frequencies around 270–340 kHz were used. According to the manufacturer, the radius of the tip was less than 10 nm. The surface of each sample was imaged in at least three different places.

2.2.6. Scanning Electron Microscopy (SEM)

SEM of freestanding CNF films and textiles was performed with a Zeiss Sigma VP (Carl Zeiss NTS Ltd, Germany) field emission scanning electron microscope using an acceleration voltage of 1.5 kV. Prior to imaging, the samples were attached to an aluminum SEM stubs with carbon tape followed by sputter-coating (Emitech K100X) with Pt/Pd forming a thin layer of ~10-15 nm to avoid charging and to enhance the signal from the sample.

2.2.7. Roughness

The roughness of QCM-D crystals after adsorption measurements and modified free standing CNF films was determined using AFM and scanning white light interference microscope (ContourGT-K, Bruker Corporation, USA), respectively. After the adsorption experiments in QCM-D, NanoScope

Analysis 1.5 software was used to calculate the arithmetical mean height S_a from the AFM height images of the coated substrates. The image size used for the S_a analysis was 25 µm^2. The arithmetical mean height S_a of the surfaces of self-standing CNF films was calculated using the on-board software of the scanning white light interference microscope. The area scanned was 423 µm x 564 µm, the focus was 20x0.55x, and each sample was measured three times.

2.2.8. Fourier transform infrared spectroscopy (FTIR)

To characterize the chemical composition of the samples FTIR spectra were measured using a Nicolet Magna IR750 Fourier transform infrared with an attenuated total reflection (ATR) accessory. The spectroscopy was performed on textiles, and each spectrum is an average of 64 measurements.

2.2.9 X-ray photoelectron spectroscopy (XPS)

Kratos Analytical AXIS Ultra electron spectrometer with monochromatic A1 Kα irradiation at 100 W was used for surface chemical analysis of fabrics. Elemental surface composition was determined from low resolution survey scans, while high resolution measurements of carbon C 1s and oxygen O 1s regions were applied for a more detailed chemical evaluation. Furthermore, nitrogen contents were evaluated using long regional N 1s scans recorded with survey resolution so that they could be incorporated into survey quantifications. 2-3 locations were measured for each sample, with nominal analysis area of 300 x 700 µm. Pure cellulose filter paper (Whatman) was used as in-situ reference with each measurement batch. CasaXPS software was utilized for data analysis, and for the carbon regions a specific four component fitting routine tailored for cellulosic specimen was used (Johansson & Campbell, 2004).

2.2.10. Oxygen Transmission Rate (OTR)

The OTR was measured with Oxygen Permeation Analyser Models 8001 and 8011 (Systech Instruments Ltd, UK) with two replicates. The tests were carried out at 23 °C and 50% and 80% RH using metal masks with a test area of 5 cm^2. Oxygen permeability (OP) was calculated by multiplying OTR value by the thickness of the sample.

2.2.11. Moisture buffering capacity

The hygroscopic behaviour of the textiles was tested in a climate chamber at 23 °C with cycles of 16 h 33% RH and 8h 75% RH. Reference textiles were tested together with two coatings: 2 bilayers of PLL/wax and 2 bilayers of PLL/wax annealed at 103 °C for 1 h. Three replicates were used for each system. The sample size was 5x5 cm and all sides were exposed. Four of the sides were of negligible size, and the samples were thin enough for the moisture to pass through them, so only one side was used to calculate the moisture buffering. Prior to testing, the samples were stabilized in the chamber for two days.

3. Results and discussion

3.1. Model studies on ultrathin CNF films

Adsorption of the PLL and wax particles on ultrathin CNF films was studied in situ with the QCM-D technique to evaluate the optimum pH conditions for the multilayer build-up. PLL was found to adsorb well on the cellulosic surface with an initial rapid increase in sensed mass, followed by slow increase in mass until a stable plateau was reached. The consequent adsorption of wax onto PLL was

even more rapid and a stable plateau was reached quicker. The adsorption kinetics are represented in Fig. 1a as the sensed mass over time. It should be noted that the sensed mass was calculated from the change in frequency and thus includes also water bound to the adsorbed layer. It was previously reported that adsorption of PLL on various substrates is controlled by the balance of electrostatic and nonelectrostatic interactions (Choi et al., 2015). In the current work, the adsorption was most likely driven by the entropy gain due to release of counterions during adsorption of oppositely charged components, but hydrophobic interactions between PLL and wax particles may have also played a role (Choi et al., 2015; Zou, Oukacine, Le Saux, & Cottet, 2010). Upon rinsing with water, a slight decrease in sensed mass of PLL was observed, likely deriving from the removal of some loosely bound molecules. Nevertheless, a substantial amount of the polymer remained adsorbed on the CNF surface even after rinsing. The consecutive adsorption of the wax particles was relatively rapid and almost no wax was removed during the rinsing step. The sensed mass of wax was much higher than that of PLL. This was expected, since the wax dispersion contained micro- and nanoparticles as opposed to PLL, that was dissolved in water and adsorbed as a thin polymer film. Additionally, the wax dispersion was adsorbed from a higher concentration than the PLL.

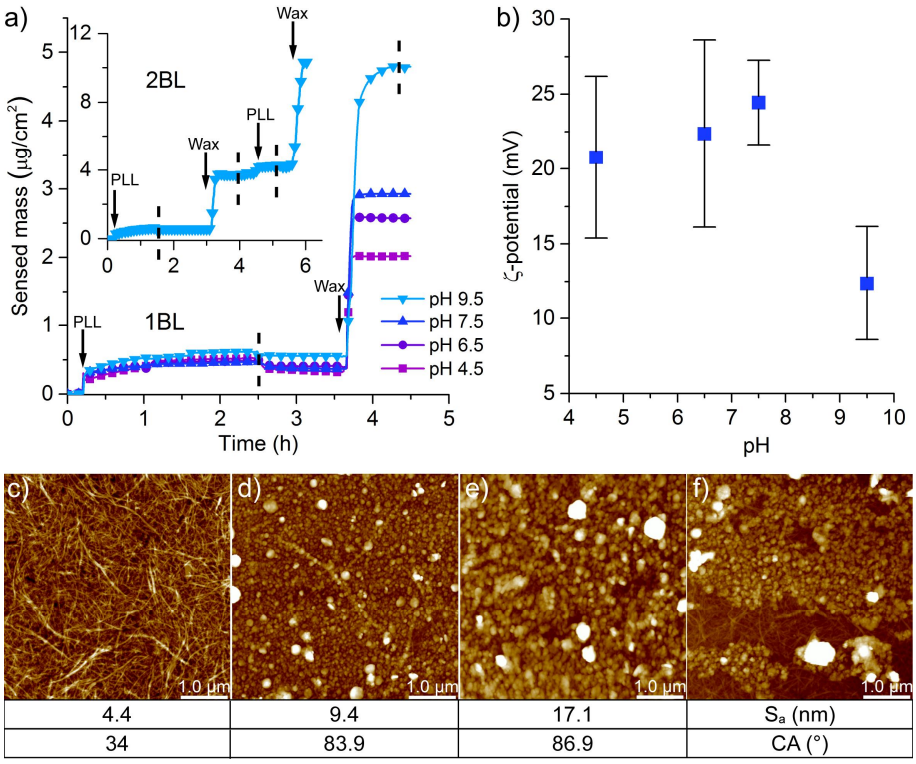

Fig. 1 (a) Effect of pH on sensed mass of PLL and wax, adsorbed as one bilayer (1BL) onto CNF surface. In the inset the sensed mass of two bilayers (2BL) of PLL at pH 9.5 and wax is shown. In both cases, only the pH of PLL solution was adjusted. Arrows on the graph indicate the injection of the adsorbate and dashed lines indicate rinsing with water. (b) Influence of pH on the ζ-potential of the PLL solution. (c-f) AFM height images, with corresponding arithmetical mean height S_a and water CA, of QCM-D crystal with pure CNF thin film (c), and CNF films with 1BL (d) and 2BL (e, f) of PLL/wax. Adsorption was done with PLL at pH 9.5 (d-f). f) highlights the cracks observed in some of the 2BL films.

The charge and the conformation of the PLL molecules are affected by the pH of the solution, thus the influence of pH on adsorption was investigated. The adsorption of both PLL and wax was found

to increase with the increase in the pH of the PLL. The adsorption was the highest at pH 9.5 for both PLL and wax, resulting in sensed mass of almost 5 μg/cm^2 per bilayer (BL) of the coating. These results are consistent with previous studies, which report that the adsorption of PLL on the surface of silica increases with the increase in pH (Porus, Maroni, & Borkovec, 2012). It was also reported that the adsorption on gold and silica was the highest in the pH range 9 to 11, when the charge density of the PLL molecule is minimal (Barrantes et al., 2012; Choi et al., 2015). When intermolecular electrostatic repulsion between PLL molecules reaches sufficiently low level, the molecules undergo conformational transition from random coil to α-helix. This transition leads to the reduction of hydrodynamic radius of the PLL structure (Choi et al., 2015; Rodríguez-Maldonado, Fernández-Nieves, & Fernández-Barbero, 2005). Their reduced size may result in enhanced diffusion rate of the PLL molecules to the surface and higher packing density during adsorption (Choi et al., 2015). Additionally, the ζ-potential of the PLL in water was clearly reduced at pH 9.5 as shown in Fig. 1b, indicating that its overall charge was lower. The reduced charge may decrease the repulsion between PLL molecules at the surface and, therefore, may have led to higher adsorbed amount. With more PLL on the surface, also more wax was adsorbed. Therefore, the PLL at pH 9.5 was chosen to be optimal for this work, as it maximizes the wax adsorption, which should have a positive impact on the hydrophobicity of the coated surfaces.

The inset in Fig. 1a shows the adsorption of two bilayers of PLL/wax with PLL at pH 9.5, suggesting that it is possible to build up more than one bilayer onto the CNF substrate. As expected, the adsorbed mass of wax is even higher for the second bilayer, possibly due to increased specific surface area of the substrate. An exponential layer growth is very often observed for LbL deposition in general (Karabulut & Wågberg, 2011), and has also been previously observed when PLL was involved in polymer multilayers (Barrantes et al., 2012; Krzeminski et al., 2006). After the deposition of the first bilayer there may be more hills and valleys on the surfaces acting as new binding sites for wax particles to attach on. However, in terms of potential industrial applications on textiles, increasing the amount of bilayers further is not economically relevant. Therefore, only 1BL and 2BL of PLL/wax coatings were studied in this work.

The morphology of QCM-D crystals coated with CNF and 1 or 2 bilayers of PLL (pH 9.5)/wax was further evaluated with AFM and topographical images are shown in Fig. 1 c-f. PLL and wax formed a coating that evenly covered the CNF fibrils. The amount of visible wax particles on the surface increased with increasing number of bilayers. After adsorption of one bilayer, the fibrils of the CNF substrate were still slightly visible (Fig. 1d), while they were fully covered with particles after the substrate was coated with two bilayers (Fig. 1e). Polyelectrolyte layers have been noted to be too even and thin to be detected on CNF using AFM (Eronen, Junka, Laine, & Österberg, 2011), thus only the topographical changes due to wax particle adsorption are discussed. Unexpectedly, on the surface that was coated with 2BL, cracks in the coating were detected in some regions, revealing the underlying cellulose nanofibrils, as seen in Fig. 1f. Cracks might be the result of drying of the coated crystal and they were only detected on crystals with the 2BL of the coating. The thicker 2BL coating may be less flexible than the thinner 1BL and thus crack upon drying. Another reason for cracking might be the hardness of the substrate (gold QCM-D crystal); with a more flexible substrate, cracking could be reduced or even avoided, as will be shown later for other cellulosic samples.

As expected, the nanoscale roughness of the surface increased with the LbL coating, as indicated by the S_a values in Fig. 1c-f. The CA of water on the substrates before and after coating is also shown in

Fig. 1c-f. The water CA of QCM-D crystal increased from 34° on pure CNF surface, to 83° and 86° for 1BL and 2BL coatings, respectively. The CA of coated crystals was still below 90°, so they cannot, strictly speaking, be classified as hydrophobic. However, considering that the samples are very flat on the micro scale, the increase in CA was still very significant.

3.2. LbL deposition on freestanding CNF films

After successful studies on model CNF surfaces, PLL/wax LbL coatings were applied onto self-standing CNF films in order to hydrophobize them and test the performance of the coating on macroscopic samples. One and two bilayers of coating were deposited onto freestanding CNF films. In order to investigate melting of the wax particles and its effect on the coating, some samples were thermally annealed in oven for one hour at 103 °C after the LbL process. Change in dry mass of the 4×4 cm CNF samples after 2BL coating was found to be 0.0001 g, which was the limit of the sensitivity of the scale and thus might not be very accurate. However, it is a good indication of the fact that the deposited coating is extremely thin. The topography of the unmodified films, the coated films, and coated and thermally annealed films is presented in Fig. 2. Both 3D 25 μm^2 images and 2D 1 μm^2 images are shown since the former shows the microscale features better, while 2D images reveal details like CNF fibrils.

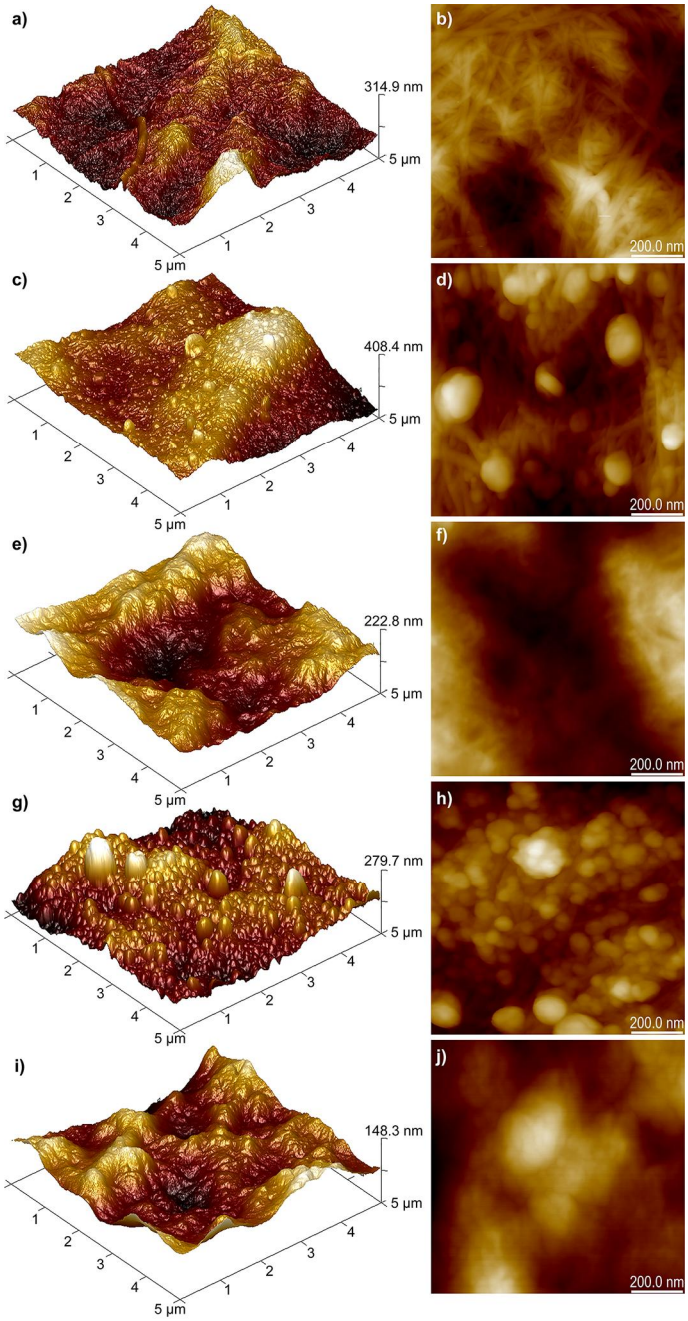

Fig. 2 Atomic force microscopy height images of freestanding CNF films. Pure CNF film (a, b), CNF films with 1BL of PLL/wax before (c, d) and after (e, f) thermal annealing, and CNF films with 2BL of PLL/wax before (g, h) and after (i, j) thermal annealing.

After the LbL coating, topographical changes on the surface of freestanding CNF films were similar to those on the surface of ultrathin CNF films that were previously reported in this work. The notable difference was the absence of the cracking of the coating layer, indicating that cracking did not occur on flexible substrates. Deposition of 1BL of PLL/wax (Fig. 2c and 2d) resulted in partial coverage of cellulose fibrils, while 2BL (Fig. 2g and 2h) covered the substrate completely, thus making the surface appear more rough. Thermal annealing of 1BL (Fig. 2e and 2f) and 2BL (Fig. 2i and 2j) coatings resulted in melting of the wax particles and consequently the surface appeared smoother. SEM images of the coated CNF films in Fig. S1 allow assessing the topography of the coated samples on a bigger scale.

The microscale roughness of the CNF films was examined in connection to their CA values (Fig. 3), because it is well known that roughness and surface energy both play an important role in controlling the wetting properties of the surface (Song & Rojas, 2013). The roughness values of the CNF films in Fig. 3 were qualitatively in good agreement with the AFM topography.

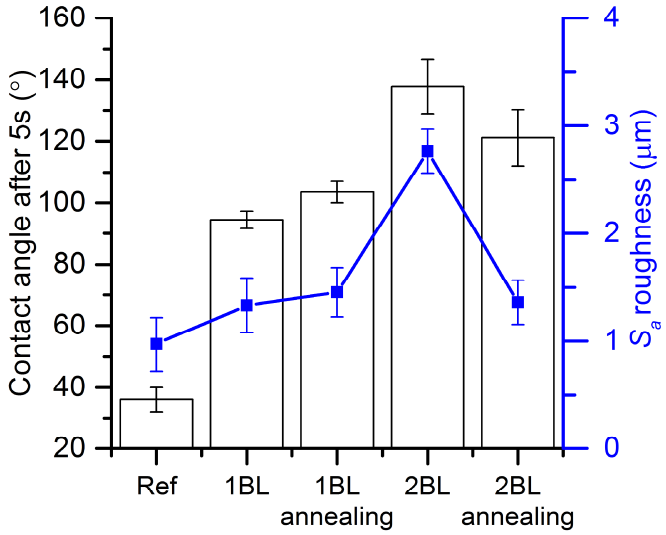

Fig. 3 Contact angle and arithmetical mean height roughness of freestanding CNF films with and without multilayer PLL/wax coating. Line on the S_a graph is provided as a guidance for the eye only.

The PLL/wax coatings efficiently hydrophobized the CNF films and increased CA from 34° to 94° after one bilayer and up to 138° after two bilayers. As seen in Fig.3, the 1BL coating increased the roughness only slightly. Therefore, the change in wetting was probably attributed to the low surface energy of the wax particles. It is noteworthy that although the surface was only partly covered with wax particles after 1BL coating, the CA changed drastically. In the literature it has also been previously demonstrated, that partial coverage is enough to significantly change the wetting properties of surfaces (Dong, Nypelö, Österberg, Laine, & Alava, 2010). Thermal annealing of the films coated with 1BL films did not have a pronounced effect on the roughness, but slightly increased the CA. This was probably due to spreading of the wax that led to a better coverage of the hydrophilic cellulose substrate with hydrophobic wax. Compared to the pure CNF reference, the 2BL coating increased the roughness of the surface almost three fold, thus the high CA of this coating can probably be associated with both the roughness of the surface as well the low surface energy of wax. Thermal annealing of the 2BL-coated surface decreased the roughness considerably, to the same level as the annealed 1BL coating, indicating melting of the wax particles. It has been shown in literature that the effect of the roughness on wettability is very pronounced (Feng & Jiang, 2006; Semal et al., 1999). Therefore, the decrease in roughness can be considered to be the reason for the slight decrease in CA as compared to the un-annealed 2BL sample. However, the CA is still higher than for annealed 1BL sample. This may be due to differences in coverage. From the AFM images in Fig. 2f and 2j it is evident that the one annealed bilayer is not fully covering the CNF substrate while two annealed bilayers seem to coat the substrate efficiently. Examples of the successful surface hydrophobization of the cellulosic films in literature already exist and include grafting at the surface and chemical modification (Chinga-Carrasco et al., 2012; Kämäräinen et al., 2016; Missoum, Sadocco, Causio, Belgacem, & Bras, 2014; Rodionova, Lenes, Eriksen, & Gregersen, 2011), coating with

paraffin wax (Österberg et al., 2013), and adsorption of surfactants (Syverud, Xhanari, Chinga-Carrasco, Yu, & Stenius, 2011). However, to the best of our knowledge, this high CA has not previously been achieved using purely natural materials. Thus, the sustainability and the simplicity of the LbL approach, along with high hydrophobicity of the coated CNF films make the developed coating rather unique.

The very densely packed fibrils make the freestanding CNF films a promising platform for the development of food packaging materials (Österberg et al., 2013). These films have very low oxygen permeability in dry conditions, but due to the hydrophilic nature of the cellulose, they do not perform very well at elevated humidity (Lozhechnikova et al., 2014). A hydrophobic coating may improve the performance of CNF films at high humidity and thus, the oxygen transmission rate was measured for the CNF films coated with thermally annealed 2BL PLL/wax coating. Only this sample was tested since for good oxygen barrier properties an impermeable, continuous layer is needed (Gupta et al., 2010). The non-perfect coverage of 1BL sample as well as the open, non-continuous structure of wax layer prior to annealing in the 2BL case was expected to decrease the barrier properties of these samples. Oxygen permeability (OP) at 80 % RH of the pure and the 2BL-coated and annealed CNF films was found to be 8.4 and 6.6 cm^3 µm m^{-2} d^{-1} kPa^{-1}, respectively, showing only a slight improvement in oxygen barrier properties. Hydrophobic surface treatments of cellulose have been previously reported to be effective at reducing the OP at elevated humidity (Österberg et al., 2013; Vartiainen & Malm, 2016). However, in the case of the current treatment, although cellulose fibrils are coated with melted layer of PLL and wax, it appears that there is still some space for oxygen to go through. No cracks or defects in the coatings were detected by AFM or SEM imaging, but the wax used for this study is quite brittle in nature. Thus, there is a possibility that cracks on nanoscale might have formed in the coating, thus reducing the effectiveness of its oxygen barrier performance. Nevertheless, the non-continuous nature of the wax particle layer is probably more beneficial for applications where it is advantageous to combine hydrophobicity with gas permeability.

3.3. LbL deposition on textiles

Typically, to achieve water resistance, fabrics are laminated with polymer coatings, such as neoprene, polyvinyl chloride or polyurethane (Mather & Wardman, 2011). These coatings not only make the fabric completely waterproof, they also make it impervious to air and very stiff. Therefore, textiles treated in such a way are more suitable for technical products rather than clothing (Mather & Wardman, 2011). As opposed to aforementioned lamination, the developed coating with PLL and wax could be used in areas where protection of the cellulosic material from water is needed, but where it is also important to retain the moisture buffering or the breathability of the material. For example, textiles for home and furniture, outdoor clothing, sports and active-wear garments.

Three natural fabrics were chosen in order to test the suitability of the coating for textiles: light cotton, heavy cotton and linen (flax). Prior to coating, all samples were washed with ethanol to remove impurities and traces of previous chemical treatments. Samples of each textile were coated with 2BL of PLL/wax coating and some were also thermally annealed after the coating. Qualitatively, the feel and the appearance of the textiles were not affected by the treatment. To evaluate the wetting of the initial and coated surfaces, CA measurements were performed on the fabrics and results are summarised in Table 1. A practical wettability demonstration is shown in Video S1 and Video S2 in the SI.

Table 1 Water CA after 5 and 30 seconds on the unmodified and coated textile surfaces. Standard deviations for CA measurements are shown in brackets.

	Light Cotton		Heavy Cotton		Linen	
Treatment	CA after 5s	CA after 30 s	CA after 5s	CA after 30 s	CA after 5s	CA after 30 s
Unmodified	<10	NA	<10	NA	<10	NA
2BL PLL/wax	140 (2.2)	140 (2)	135 (3.9)	NA	146 (5.5)	143 (4.4)
2BL PLL/wax annealed	156 (6.8)	156 (7.4)	149 (5.8)	148 (6.1)	139 (3.3)	138 (3.2)

As can be seen from the Table 1, all tested textiles became highly hydrophobic after the coating with 2BL of PLL/wax. The change in wetting after just two bilayers of coating was drastic, considering that uncoated textile samples adsorbed the water drops within the first few seconds. The long-term water-repelling performance of the surfaces was evaluated qualitatively, since the small water droplets used for CA measurements evaporate with time. The photographs in Fig. 4 show water droplets on coated textiles after three hours of contact, illustrating that the treatment led to long lasting water resistance.

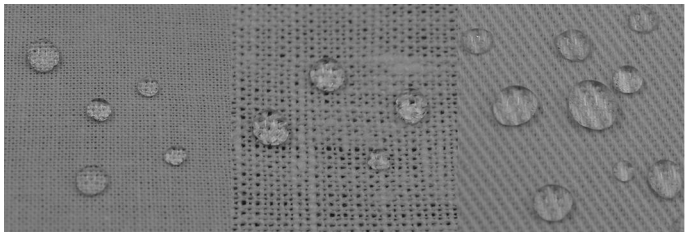

Fig. 4 Water droplets after three hours on textiles coated with 2 BL PLL/wax and annealed. From left to right the samples are light cotton, linen and heavy cotton.

Correlation can be found between the CA of coated textiles and their surface coverage with particles as seen in SEM images (Fig. 5). The amount of wax particles at the surface of 2BL-coated linen (Fig. 5 c2) was much higher than that of the cotton samples (Fig. 5 a2, b2). High surface coverage with wax and the additional roughening that these particles bring may be the reason for the very high CA values of linen before annealing. Overall, the coated textiles exhibited higher CA than the coated freestanding CNF films. Similarly, the freestanding films had higher CA in comparison to the QCM-crystals. This can be explained by the difference in roughness of the substrates, with higher roughness contributing to higher CA values.

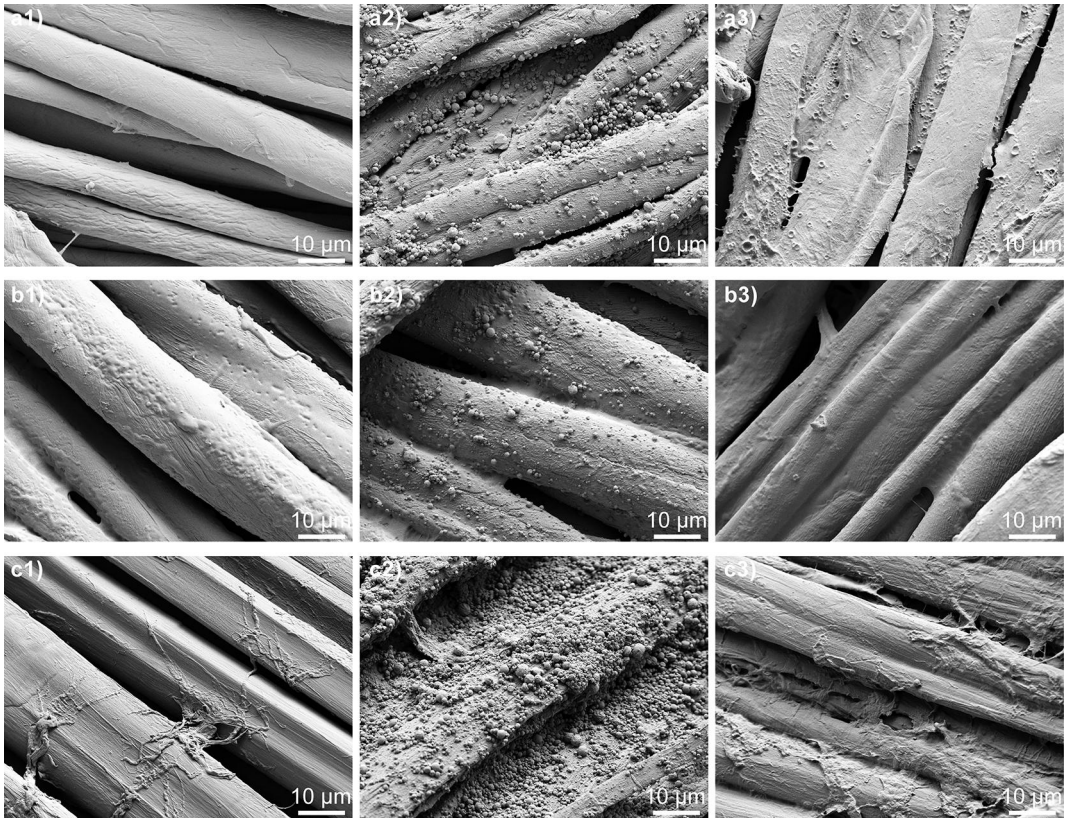

Fig. 5 SEM images of light cotton fabric before coating (a1), coated with 2BL (a2), and coated and annealed (a3); heavy cotton fabric before coating (b1), coated with 2BL (b2), coated and annealed (b3); linen fabric reference (c1), coated with 2BL (c2), and coated and annealed (c3).

Raw cotton and flax fibres are known to have substantial amounts of surface contaminants covering cellulose, such as waxes, pectins, extractives and lignin (Rippon & Evans, 2012). Most of these contaminates are removed during scouring and bleaching of the fibres, but some part of them might still remain bound to the fibre surface (Mitchell, Carr, Parfitt, Vickerman, & Jones, 2005). It has also been reported that even after the acetone extraction of fibres, the surface coverage with extractives and waxes is higher on cotton than on flax (Buchert, Pere, Johansson, & Campbell, 2001). It is important to note that textiles purchased for this work were commercially available fabrics and the kind of treatments they were subjected to during production is not known. To evaluate the purity of the cellulosic fabrics and the effect of the PLL-wax coatings ATR-FTIR and XPS were used (Fig. 6, S3 and S4).

The FTIR spectra of the unmodified samples (Fig. S3) are similar to the spectrum of native cellulose (Dlouhá, Suryanegara, & Yano, 2012). However, the heavy cotton sample had an additional band around 1700 cm^{-1}, suggesting traces of C=O groups on the surface. This band might originate from a chemical treatment (i.e. acetylation) or impurities, and it does not occur in the other reference samples. This may explain the visually poorer surface coverage of the heavy cotton sample with the PLL/wax coating. The cationic PLL is expected to adsorb the most on a very clean cellulose surface and the more PLL the more wax is adsorbed. There is some noise in the 1900-2400 cm^{-1} region in all spectra, which is caused by CO_2 and the diamond used in the measuring. The XPS data (S4 in Supporting Information) further confirms that the heavy cotton sample was not pure cellulose. It

showed a clearly stronger C-C signal and higher surface nitrogen content than the other reference samples.

The effect of the coating and annealing on the FTIR spectra for all textile samples can be seen in Fig. S3. The carnauba wax in the coated samples can be identified by the methylene vibration at 2919 cm^{-1} and 2848 cm^{-1} (stretching) (Ribeiro da Luz, 2006). These peaks were most prominent in the 2BL samples, and they decreased after the thermal annealing, probably due to melting of the coating and its penetration between the fibres.

XPS spectra of the outermost surface of the linen samples further corroborates this conclusion (Fig. 6 and Table 2). We note that the band originating from carbon atoms bound to only other carbon atoms or hydrogen (C-C) dominates the high-resolution spectrum of the carbon band for both PLL/wax treated samples. This signal originates from the wax, suggesting a very high surface coverage of wax. The C-C band was highest for the annealed sample. Interestingly, the relative surface concentration of nitrogen was the highest, 0.9% for the 2BL sample prior to annealing, compared to only 0.2% after annealing. The nitrogen band origins from the PLL and together these results suggest that before annealing the wax particles are abundant but do not fully cover the surface, both nitrogen from PLL and C2 and C3 bands from cellulose are observed. The annealing leads to melting of the wax particles forming a fully covering wax film.

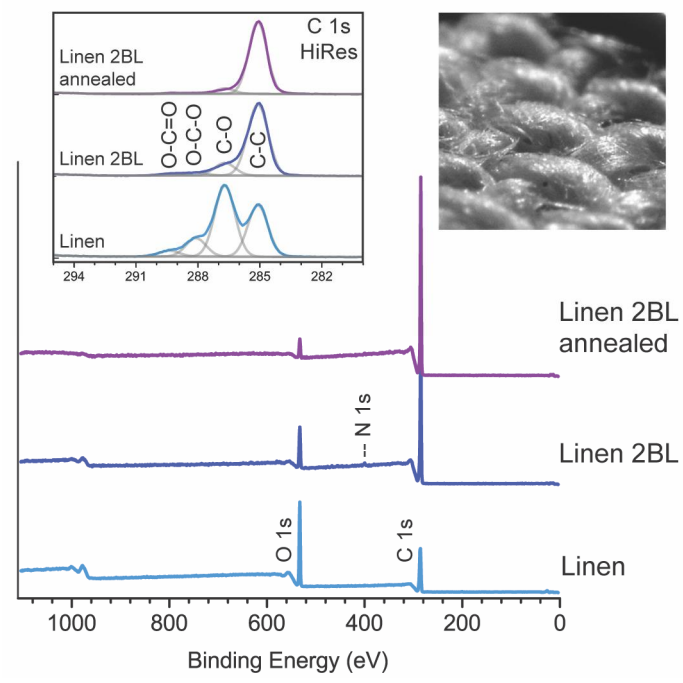

Fig. 6 High resolution XPS spectra of untreated, coated, and coated and annealed linen. The included photo is the optical picture captured from camera in XPS apparatus, viewing untreated linen

Table 2 Wide atomic concentrations and high resolution C 1s carbon fits of untreated reference samples and coated, and coated and annealed linen. Values are given in atomic percentage, as average of two measurements, except for untreated linen that the average of three measurements.

	Wide atomic concentrations (atomic %)			High resolution C 1s carbon fits (atomic %)			
Treatment	C 1s	O 1s	N 1s	CC	CO	COO	COOO

light cotton unmodified	69.5 %	30.3 %	0.2 %	32.0 %	50.9 %	12.7 %	4.4 %
heavy cotton unmodified	73.1 %	26.4 %	0.5 %	41.2 %	42.4 %	6.7 %	9.7 %
linen unmodified	70.2 %	29.6 %	0.2 %	33.4 %	49.4 %	13.3 %	3.8 %
linen 2BL PLL/wax	91.4 %	7.7 %	0.9 %	81.1 %	13.8 %	3.0 %	2.2 %
linen 2BL PLL/wax annealed	96.6 %	3.1 %	0.2 %	91.3 %	6.8 %	0.9 %	0.9 %

Consecutive thermal treatment was the most beneficial for cotton samples. After the annealing, CA of the light cotton and heavy cotton samples increased up to 156° and 149° respectively. With CA of around 150°, both samples could thus be considered superhydrophobic. It is not clear why the thermal treatment was more beneficial for cotton than for flax fibres in terms of reduction of their wetting with water. As can be observed from SEM images, the roughening after 2BL of coating is the most pronounced on the surface of flax fibres. Therefore, the decrease in nano- and microscale roughness upon annealing may be one reason for the lower CA of linen. However, due to the fibrillar nature of the fabrics (Fig. 6), it was not possible to accurately measure the roughness of the textile samples using scanning white light interference microscope. In the case of cotton samples, increase in CA after the annealing might originate from the better surface coverage with melted wax due to the film formation. Clearly, both high enough coverage of low surface energy wax and roughness are necessary for high hydrophobicity. Nevertheless, it is noteworthy that all treated samples had a remarkable increase in contact angle, considering the very thin coating layer.

High hydrophobicity is an indisputable advantage for a textile in many applications, but just hydrophobicity is often not enough. For example, in clothing, comfort has become an important consideration and in order to provide it, breathability of the material is required (Mukhopadhyay & Vinay Kumar, 2008). The ability of the water vapour to penetrate through the material is therefore crucial even for hydrophobic textiles. As was reported earlier in this work, at high level of RH the annealed 2BL coating did not significantly affect the oxygen transmission through the CNF films. Therefore, it could be expected that the coating would not prevent the airflow through the fabrics either. No tests were performed on CNF films regarding the water vapour permeation and therefore, the ability of the textile samples to adsorb and release moisture was evaluated. The procedure for the breathability testing of the hydrophobic textiles is a matter of controversy and confusion and a universal method is yet to be found (Lomax, 2007). Thus, a simple procedure was chosen, where textiles were exposed to changes in relative humidity and their mass was monitored. When subjected to 75% RH, untreated fabrics and fabrics coated with 2BL, adsorbed moisture, as indicated by the increase in mass in Fig. S2. When RH was lowered to 33%, the samples lost some of the weight due to moisture desorption. Average moisture adsorption and desorption upon changing the RH between 75 and 33% was 4.5, 7.8 and 8.7 g/m^2 for light cotton, heavy cotton, and linen. The grammage of the linen and heavy cotton was almost twice as high as that of the light cotton, so the higher water vapour adsorption was expected. Comparing to the untreated fabrics, the 2BL coating reduced moisture adsorption and desorption by 16% for lightweight cotton, and by 5% and 4% for heavy cotton and linen, respectively. As expected, due to the partial melting of the wax particles during annealing, the thermal treatment further reduced the moisture sorption and release. Comparing to the untreated fabrics, the annealed coating reduced the amount of adsorbed and desorbed moisture by 38, 11 and 20% for light cotton, heavy cotton, and linen, respectively. However, as can be seen on Fig. S2, even after the annealing of the coated textiles, they were still able to adsorb and desorb moisture as the surrounding humidity conditions changed. The fact that

the hygroscopic nature of the natural textiles was preserved despite the very high hydrophobicity of the treated samples, makes the multilayer coatings with PLL and natural wax a very promising route for many applications.

Fabrics with this multilayer coating could be used as domestic or as wearable textiles. Indoor they can help to reduce extremes in relative humidity, while in clothing they would allow for sweat and excess moisture to be transported from the body. Clothes made of such hydrophobic textiles would be water-repellent, but at the same time breathable and thus comfortable. The concept of the breathable hydrophobic textile is not particularly new and many products are already available that utilize various technologies, including examples of closely woven or laminated fabrics, microporous membranes and nano- finishings. (Mukhopadhyay & Kumar, 2008) However, the developed PLL/wax coating has several advantages over the existing solutions. Firstly, it is applicable to natural cellulosic materials, in contrast to the majority of existing solutions that use synthetic fibres. Furthermore, its simple water-based LbL procedure, absence of organic solvents or fluorine-containing compounds, as well as excellent hydrophobicity of the final product, make it a very promising treatment for cellulosic materials, including various films and textiles.

4. Conclusions

In this work, cellulosic fabrics and thin freestanding CNF films were coated with poly-L-lysine and carnauba wax bilayers. The coating made CNF surfaces and textiles highly hydrophobic, while consecutive thermal treatment lead to melting of the wax particles, which in some cases increased the hydrophobicity even further. Superhydrophobicity was achieved on cotton fabric, with CA reaching up to 156°. The water resistance was long-lasting and water droplets did not absorb into the fabric or spread on the surface for many hours. The increase in roughness from ultrathin CNF films to freestanding CNF films and especially textiles is significant, and can probably explain the superior hydrophobicity of coated textiles compared to the films. Coated CNF films still allowed oxygen permeation at high RH, even after the annealing at 103°C. Thus, they would probably be best suited for applications where it is advantageous to combine hydrophobicity with gas permeability. In the case of textiles, the PLL/wax coatings reduced their water-vapour sorption properties only slightly, and they were still able to adsorb and desorb moisture. Furthermore, the moisture buffering ability of the fabrics was preserved even after melting and film-formation of the coating.

The open, rough coating obtained using natural wax particles, made cellulose materials hydrophobic yet breathable, which could be very promising for many applications, e.g. packaging, domestic and wearable textiles. While non-renewable fabrics dominate the global textile market, the use of natural textiles could benefit the indoor climate and result in more breathable and comfortable clothing. A coating that enhances the properties of natural textiles can give them a huge advantage versus synthetic fibres, and thus help moving towards a more sustainable, eco-friendly society.

Acknowledgements

Aalto Energy Efficiency Research Programme is acknowledged for funding through the Wood Life Project. This work made use of Aalto University Nanomicroscopy Center (Aalto-NMC) and Bioeconomy facilities. Österberg acknowledges Academy of Finland project number 278279.

References

Badanova, A. K., Taussarova, B. R., & Kutzhanova, A. Z. (2014). Hydrophobic finishing of cellulosic

textile material. *World Applied Sciences Journal*, *30*(10), 1409–1416. https://doi.org/10.5829/idosi.wasj.2014.30.10.14188

Barrantes, A., Santos, O., Sotres, J., & Arnebrant, T. (2012). Influence of pH on the build-up of poly-L-lysine/heparin multilayers. *Journal of Colloid and Interface Science*, *388*(1), 191–200. https://doi.org/10.1016/j.jcis.2012.08.008

Bayer, I. S., Fragouli, D., Martorana, P. J., Martiradonna, L., Cingolani, R., & Athanassiou, A. (2011). Solvent resistant superhydrophobic films from self-emulsifying carnauba wax-alcohol emulsions. *Soft Matter*, *7*(18), 7939–7943. https://doi.org/10.1039/c1sm05710c

Brown, P. J., & Stevens, K. (2007). Nanofibers and nanotechnology in textiles. In *Nanofibers and Nanotechnology in Textiles* (pp. 1–528). Retrieved from https://www.scopus.com/inward/record.uri?eid=2-s2.0-84903499897&partnerID=40&md5=2261a20c2f35790f1f379633f12249f6

Buchert, J., Pere, J., Johansson, L. S., & Campbell, J. M. (2001). Analysis of the surface chemistry of linen and cotton fabrics. *Textile Research Journal*, *71*(7), 626–629. Retrieved from https://www.scopus.com/inward/record.uri?eid=2-s2.0-0035391029&partnerID=40&md5=ef96c5b0e6645d069eeb1d76960aaec7

Chang, J., Zhong, Z., & Xu, H. (2012). Multifunctional wool fiber treated with e-polylysine. *Korean Journal of Chemical Engineering*, *29*(4), 507–512. https://doi.org/10.1007/s11814-011-0194-2

Chen, X., Fang, F., Zhang, X., Ding, X., Wang, Y., Chen, L., & Tian, X. (2016). Flame-retardant, electrically conductive and antimicrobial multifunctional coating on cotton fabric via layer-by-layer assembly technique. *RSC Advances*, *6*(33), 27669–27676. https://doi.org/10.1039/c5ra26914h

Chinga-Carrasco, G., Kuznetsova, N., Garaeva, M., Leirset, I., Galiullina, G., Kostochko, A., & Syverud, K. (2012). Bleached and unbleached MFC nanobarriers: Properties and hydrophobisation with hexamethyldisilazane. *Journal of Nanoparticle Research*, *14:1280*. https://doi.org/10.1007/s11051-012-1280-z

Choi, J. H., Kim, S. O., Linardy, E., Dreaden, E. C., Zhdanov, V. P., Hammond, P. T., & Cho, N. J. (2015). Influence of pH and Surface Chemistry on Poly(l -lysine) Adsorption onto Solid Supports Investigated by Quartz Crystal Microbalance with Dissipation Monitoring. *Journal of Physical Chemistry B*, *119*(33), 10554–10565. https://doi.org/10.1021/acs.jpcb.5b01553

CIRFS. (2016). World Man-Made Fibres Production. Retrieved February 1, 2017, from http://www.cirfs.org/KeyStatistics/WorldManMadeFibresProduction.aspx

Cranston, E. D., & Gray, D. G. (2006). Morphological and optical characterization of polyelectrolyte multilayers incorporating nanocrystalline cellulose. *Biomacromolecules*, *7*(9), 2522–2530. https://doi.org/10.1021/bm0602886

Cranston, E. D., Gray, D. G., & Rutland, M. W. (2010). Direct surface force measurements of polyelectrolyte multilayer films containing nanocrystalline cellulose. *Langmuir*, *26*(22), 17190–17197. https://doi.org/10.1021/la1030729

Decher, G., Hong, J. D., & Schmitt, J. (1992). Buildup of ultrathin multilayer films by a self-assembly process: III. Consecutively alternating adsorption of anionic and cationic polyelectrolytes on charged surfaces. *Thin Solid Films*, *210–211*(PART 2), 831–835. https://doi.org/10.1016/0040-6090(92)90417-A

Deng, B., Cai, R., Yu, Y., Jiang, H., Wang, C., Li, J., ... Fan, C. (2010). Laundering durability of superhydrophobic cotton fabric. *Advanced Materials*, *22*(48), 5473–5477.

https://doi.org/10.1002/adma.201002614

Dlouhá, J., Suryanegara, L., & Yano, H. (2012). The role of cellulose nanofibres in supercritical foaming of polylactic acid and their effect on the foam morphology. *Soft Matter*, *8*(33), 8704. https://doi.org/10.1039/c2sm25909e

Dong, L., Nypelö, T., Österberg, M., Laine, J., & Alava, M. (2010). Modifying the wettability of surfaces by nanoparticles: Experiments and modeling using the wenzel law. *Langmuir*, *26*(18), 14563–14566. https://doi.org/10.1021/la101934t

Dubas, S. T., Kumlangdudsana, P., & Potiyaraj, P. (2006). Layer-by-layer deposition of antimicrobial silver nanoparticles on textile fibers. *Colloids and Surfaces A: Physicochemical and Engineering Aspects*, *289*(1–3), 105–109. https://doi.org/10.1016/j.colsurfa.2006.04.012

Eronen, P., Junka, K., Laine, J., & Österberg, M. (2011). Interaction between water-soluble polysaccharides and native nanofibrillar cellulose thin films. *BioResources*, *6*(4), 4200–4217. Retrieved from https://www.scopus.com/inward/record.uri?eid=2-s2.0-84856434871&partnerID=40&md5=bb25202aa36af50bece941ee42c36bc0

Eronen, P., Laine, J., Ruokolainen, J., & Österberg, M. (2012). Comparison of Multilayer Formation Between Different Cellulose Nanofibrils and Cationic Polymers. *Journal of Colloid and Interface Science*, *373*(1), 84–93. https://doi.org/10.1016/j.jcis.2011.09.028

Eurostat. (2016). Packaging waste statistics. Retrieved from http://ec.europa.eu/eurostat/statistics-explained/index.php/Packaging_waste_statistics

Feng, X., & Jiang, L. (2006). Design and creation of superwetting/antiwetting surfaces. *Advanced Materials*, *18*(23), 3063–3078. Retrieved from http://www.scopus.com/inward/record.url?eid=2-s2.0-33846133206&partnerID=40&md5=0c79fccaecd5b0f994d56cacfb18267c

Gao, Q., Zhu, Q., Guo, Y., & Yang, C. Q. (2009). Formation of highly hydrophobic surfaces on cotton and polyester fabrics using silica sol nanoparticles and nonfluorinated alkylsilane. *Industrial and Engineering Chemistry Research*, *48*(22), 9797–9803. https://doi.org/10.1021/ie9005518

Glinel, K., Prevot, M., Krustev, R., Sukhorukov, G. B., Jonas, A. M., & Möhwald, H. (2004). Control of the water permeability of polyelectrolyte multilayers by deposition of charged paraffin particles. *Langmuir*, *20*(12), 4898–4902. https://doi.org/10.1021/la036078l

Gomes, A. P., Mano, J. F., Queiroz, J. A., & Gouveia, I. C. (2012). Layer-by-Layer Deposition of Antibacterial Polyelectrolytes on Cotton Fibres. *Journal of Polymers and the Environment*, *20*(4), 1084–1094. https://doi.org/10.1007/s10924-012-0507-5

Gupta, M., Lin, Y., Deans, T., Baer, E., Hiltner, A., & Schiraldi, D. A. (2010). Structure and gas barrier properties of poly(propylene- graft -maleic anhydride)/phosphate glass composites prepared by microlayer coextrusion. *Macromolecules*, *43*(9). https://doi.org/10.1021/ma100391u

Gustafsson, E., Larsson, P. A., & Wågberg, L. (2012). Treatment of cellulose fibres with polyelectrolytes and wax colloids to create tailored highly hydrophobic fibrous networks. *Colloids and Surfaces A: Physicochemical and Engineering Aspects*, *414*, 415–421. https://doi.org///dx.doi.org/10.1016/j.colsurfa.2012.08.042

Horrocks, A. R., & Anand, S. C. (2015). Handbook of Technical Textiles: Second Edition. In *Handbook of Technical Textiles: Second Edition* (Vol. 1, pp. 1–372). Retrieved from https://www.scopus.com/inward/record.uri?eid=2-s2.0-84966800422&partnerID=40&md5=74b46565bafeca3053270109bfe0c415

Jenck, J. F., Agterberg, F., & Droescher, M. J. (2004). Products and processes for a sustainable chemical industry: A review of achievements and prospects. *Green Chemistry*, *6*(11), 544–556. https://doi.org/10.1039/b406854h

Johannsmann, D., Mathauer, K., Wegner, G., & Knoll, W. (1992). Viscoelastic properties of thin films probed with a quartz-crystal resonator. *Physical Review B*, *46*(12), 7808–7815. https://doi.org/10.1103/PhysRevB.46.7808

Johansson, L. S., & Campbell, J. M. (2004). Reproducible XPS on biopolymers: Cellulose studies. In *Surface and Interface Analysis* (Vol. 36, pp. 1018–1022). https://doi.org/10.1002/sia.1827

Kalia, S., Thakur, K., Celli, A., Kiechel, M. A., & Schauer, C. L. (2013). Surface modification of plant fibers using environment friendly methods for their application in polymer composites, textile industry and antimicrobial activities: A review. *Journal of Environmental Chemical Engineering*, *1*(3), 97–112. https://doi.org/10.1016/j.jece.2013.04.009

Kämäräinen, T., Arcot, L. R., Johansson, L. S., Campbell, J., Tammelin, T., Franssila, S., … Rojas, O. J. (2016). UV-ozone patterning of micro-nano fibrillated cellulose (MNFC) with alkylsilane self-assembled monolayers. *Cellulose*, *23*(3), 1847–1857. https://doi.org/10.1007/s10570-016-0942-x

Karabulut, E., & Wågberg, L. (2011). Design and characterization of cellulose nanofibril-based freestanding films prepared by layer-by-layer deposition technique. *Soft Matter*, *7*, 3467–3474. https://doi.org/10.1039/c0sm01355b

Kotov, N. A., Dekany, I., & Fendler, J. H. (1995). Layer-by-layer self-assembly of polyelectrolyte-semiconductor nanoparticle composite films. *Journal of Physical Chemistry*, *99*(35), 13065–13069. Retrieved from https://www.scopus.com/inward/record.uri?eid=2-s2.0-0029354796&partnerID=40&md5=4431adab3d4aab67935d04c349aadb9c

Krzeminski, A., Marudova, M., Moffat, J., Noel, T. R., Parker, R., Wellner, N., & Ring, S. G. (2006). Deposition of pectin/poly-L-lysine multilayers with pectins of varying degrees of esterification. *Biomacromolecules*, *7*(2), 498–506. https://doi.org/10.1021/bm0507249

Lavoine, N., Desloges, I., Dufresne, A., & Bras, J. (2012). Microfibrillated cellulose - Its barrier properties and applications in cellulosic materials: A review. *Carbohydrate Polymers*, *90*(2), 735–764. https://doi.org/10.1016/j.carbpol.2012.05.026

Liu, Y., Tang, J., Wang, R., Lu, H., Li, L., Kong, Y., … Xin, J. H. (2007). Artificial lotus leaf structures from assembling carbon nanotubes and their applications in hydrophobic textiles. *Journal of Materials Chemistry*, *17*(11), 1071–1078. https://doi.org/10.1039/b613914k

Lomax, G. R. (2007). Breathable polyurethane membranes for textile and related industries. *Journal of Materials Chemistry*, *17*(27), 2775–2784. https://doi.org/10.1039/b703447b

Lozhechnikova, A., Bellanger, H., Michen, B., Burgert, I., & Österberg, M. (2017). Surfactant-free carnauba wax dispersion and its use for layer-by-layer assembled protective surface coatings on wood. *Applied Surface Science*, *396*, 1273–1281. https://doi.org/10.1016/j.apsusc.2016.11.132

Lozhechnikova, A., Dax, D., Vartiainen, J., Willför, S., Xu, C., & Österberg, M. (2014). Modification of nanofibrillated cellulose using amphiphilic block-structured galactoglucomannans. *Carbohydrate Polymers*, *110*. https://doi.org/10.1016/j.carbpol.2014.03.087

Lozhechnikova, A., Vahtikari, K., Hughes, M., & Österberg, M. (2015). Toward energy efficiency through an optimized use of wood: The development of natural hydrophobic coatings that retain moisture-buffering ability. *Energy and Buildings*, *105*.

https://doi.org/10.1016/j.enbuild.2015.07.052

Mather, R. R., & Wardman, R. H. (2011). *The chemistry of textile fibres*. Cambridge: RSC Publishing.

Missoum, K., Sadocco, P., Causio, J., Belgacem, M. N., & Bras, J. (2014). Antibacterial activity and biodegradability assessment of chemically grafted nanofibrillated cellulose. *Materials Science and Engineering: C*, *45*, 477–483. https://doi.org///dx.doi.org/10.1016/j.msec.2014.09.037

Mitchell, R., Carr, C. M., Parfitt, M., Vickerman, J. C., & Jones, C. (2005). Surface chemical analysis of raw cotton fibres and associated materials. *Cellulose*, *12*(6), 629–639. https://doi.org/10.1007/s10570-005-9000-9

Mukhopadhyay, A., & Vinay Kumar, M. (2008). A review on designing the waterproof breathable fabrics part I: Fundamental principles and designing aspects of breathable fabrics. *Journal of Industrial Textiles*, *37*(3), 225–262. https://doi.org/10.1177/1528083707082164

Naderi, A., & Claesson, P. M. (2006). Adsorption properties of polyelectrolyte-surfactant complexes on hydrophobic surfaces studied by QCM-D. *Langmuir*, *22*(18), 7639–7645. https://doi.org/10.1021/la061118h

Österberg, M., Vartiainen, J., Lucenius, J., Hippi, U., Seppälä, J., Serimaa, R., & Laine, J. (2013). A fast method to produce strong NFC films as a platform for barrier and functional materials. *ACS Applied Materials and Interfaces*, *5*(11), 4640–4647. https://doi.org/10.1021/am401046x

Picart, C., Lavalle, P., Hubert, P., Cuisinier, F. J. G., Decher, G., Schaaf, P., & Voegel, J.-C. (2001). Buildup mechanism for poly(L-lysine)/hyaluronic acid films onto a solid surface. *Langmuir*, *17*(23), 7414–7424. https://doi.org/10.1021/la010848g

Porus, M., Maroni, P., & Borkovec, M. (2012). Structure of adsorbed polyelectrolyte monolayers investigated by combining optical reflectometry and piezoelectric techniques. *Langmuir*, *28*(13), 5642–5651. https://doi.org/10.1021/la204855j

Qi, H., Sui, K., Ma, Z., Wang, D., Sun, X., & Lu, J. (2002). Polymeric fluorocarbon-coated polyester substrates for waterproof breathable fabrics. *Textile Research Journal*, *72*(2), 93–97. Retrieved from https://www.scopus.com/inward/record.uri?eid=2-s2.0-0036473865&partnerID=40&md5=89ddc5be017ea85498e323d5de2eecc3

Ribeiro da Luz, B. (2006). Attenuated total reflectance spectroscopy of plant leaves: a tool for ecological and botanical studies. *New Phytologist*, *172*(2), 305–318. https://doi.org/10.1111/j.1469-8137.2006.01823.x

Rippon, J. A., & Evans, D. J. (2012). Improving the properties of natural fibres by chemical treatments. In R. Kozlowski (Ed.), *Handbook of Natural Fibres* (Vol. 2, pp. 63–140). https://doi.org/10.1016/B978-1-84569-698-6.50003-6

Rodionova, G., Lenes, M., Eriksen, Ø., & Gregersen, Ø. (2011). Surface chemical modification of microfibrillated cellulose: Improvement of barrier properties for packaging applications. *Cellulose*, *18*(1), 127–134. https://doi.org/10.1007/s10570-010-9474-y

Rodríguez-Maldonado, L., Fernández-Nieves, A., & Fernández-Barbero, A. (2005). Dynamic light scattering from high molecular weight poly-L-lysine molecules. *Colloids and Surfaces A: Physicochemical and Engineering Aspects*, *270–271*(1–3), 335–339. https://doi.org/10.1016/j.colsurfa.2005.09.003

Schultz, M. M., Barofsky, D. F., & Field, J. A. (2003). Fluorinated alkyl surfactants. *Environmental Engineering Science*, *20*(5), 487–501. Retrieved from https://www.scopus.com/inward/record.uri?eid=2-s2.0-

0141828299&partnerID=40&md5=0d51ba8fba003bd5b2bc381a81551943

Semal, S., Blake, T. D., Geskin, V., De Ruijter, M. J., Castelein, G., & De Coninck, J. (1999). Influence of surface roughness on wetting dynamics. *Langmuir*, *15*(25), 8765–8770. Retrieved from https://www.scopus.com/inward/record.uri?eid=2-s2.0-0000670325&partnerID=40&md5=0fe47cb4b271a30b9f0adda3d4d9667b

Shirvan, A. R., Nejad, N. H., & Bashari, A. (2014). Antibacterial finishing of cotton fabric via the chitosan/TPP self-assembled nano layers. *Fibers and Polymers*, *15*(9), 1908–1914. https://doi.org/10.1007/s12221-014-1908-y

Song, J., & Rojas, O. J. (2013). Approaching super-hydrophobicity from cellulosic materials: A review. *Nordic Pulp and Paper Research Journal*, *28*(2), 216–238. Retrieved from https://www.scopus.com/inward/record.uri?eid=2-s2.0-84882950790&partnerID=40&md5=ef49b9622b3f6d5821d85cda3b05c569

Spence, K. L., Venditti, R. A., Rojas, O. J., Pawlak, J. J., & Hubbe, M. A. (2011). Water vapor barrier properties of coated and filled microfibrillated cellulose composite films. *BioResources*, *6*(4), 4370–4388. Retrieved from https://www.scopus.com/inward/record.uri?eid=2-s2.0-84856505370&partnerID=40&md5=920e29d331cd023a7c2a349a322fb125

Swerin, A., Odberg, L., & Lindström, T. (1990). Deswelling of hardwood kraft pulp fibers by cationic polymers. The effect on wet pressing and sheet properties. *Nordic Pulp & Paper Research Journal*, *5*(4), 188–196.

Syverud, K., Xhanari, K., Chinga-Carrasco, G., Yu, Y., & Stenius, P. (2011). Films made of cellulose nanofibrils: Surface modification by adsorption of a cationic surfactant and characterization by computer-assisted electron microscopy. *Journal of Nanoparticle Research*, *13*(2), 773–782. https://doi.org/10.1007/s11051-010-0077-1

The European Chemical Industry Council, (CEFIC). (2014). *Measuring Bio-Based raw materials use in the chemical industry*. Retrieved from http://cefic-staging.amaze.com/Documents/PolicyCentre/Industrial Policy/Measuring-Bio-based-raw-materials-use-in-the-chemical-industry-2014-03-19.pdf

Tsafack, M. J., & Levalois-Grützmacher, J. (2007). Towards multifunctional surfaces using the plasma-induced graft-polymerization (PIGP) process: Flame and waterproof cotton textiles. *Surface and Coatings Technology*, *201*(12), 5789–5795. https://doi.org/10.1016/j.surfcoat.2006.10.027

Vartiainen, J., & Malm, T. (2016). Surface hydrophobization of CNF films by roll-to-roll HMDSO plasma deposition. *Journal of Coatings Technology Research*, 1–5. https://doi.org/10.1007/s11998-016-9833-1

Xing, T., Li, X., Guo, S., Tang, R. C., Cai, J. H., & Zhou, S. Q. (2015). Preparation and properties of silk fabric grafted with ε-polylysine by tyrosinase. *Textile Research Journal*, *85*(16), 1743–1748. https://doi.org/10.1177/0040517515576323

Xu, B., & Cai, Z. (2008). Fabrication of a superhydrophobic ZnO nanorod array film on cotton fabrics via a wet chemical route and hydrophobic modification. *Applied Surface Science*, *254*(18), 5899–5904. https://doi.org///dx.doi.org/10.1016/j.apsusc.2008.03.160

Xu, B., Cai, Z., Wang, W., & Ge, F. (2010). Preparation of superhydrophobic cotton fabrics based on SiO2 nanoparticles and ZnO nanorod arrays with subsequent hydrophobic modification. *Surface and Coatings Technology*, *204*(9–10), 1556–1561. https://doi.org/10.1016/j.surfcoat.2009.09.086

Xue, C. H., Jia, S. T., Zhang, J., & Tian, L. Q. (2009). Superhydrophobic surfaces on cotton textiles by

complex coating of silica nanoparticles and hydrophobization. *Thin Solid Films*, *517*(16), 4593–4598. https://doi.org/10.1016/j.tsf.2009.03.185

Yu, M., Gu, G., Meng, W. D., & Qing, F. L. (2007). Superhydrophobic cotton fabric coating based on a complex layer of silica nanoparticles and perfluorooctylated quaternary ammonium silane coupling agent. *Applied Surface Science*, *253*(7), 3669–3673. https://doi.org/10.1016/j.apsusc.2006.07.086

Zou, T., Oukacine, F., Le Saux, T., & Cottet, H. (2010). Neutral coatings for the study of polycation/multicharged anion interactions by capillary electrophoresis: Application to dendrigraft poly-l-lysines with negatively multicharged molecules. *Analytical Chemistry*, *82*(17), 7362–7368. https://doi.org/10.1021/ac101473g

Supporting information

Layer-by-layer assembled hydrophobic coatings for cellulose nanofibril films and textiles, made of polylysine and natural wax particles.

Nina Forsman,[a,‡] Alina Lozhechnikova,[a,‡] Alexey Khakalo,[a] Leena-Sisko Johansson,[a] Jari Vartiainen[b] and Monika Österberg[a,*]

[a] *Department of Bioproducts and Biosystems, School of Chemical Engineering, Aalto University, P.O. Box 16300, FI-00076 Aalto, Finland*

[b] *VTT Technical Research Centre of Finland Ltd, Biologinkuja 7, P.O. Box 1000, FI-02044 Espoo, Finland*

*Corresponding author: Monika Österberg (monika.osterberg@aalto.fi).

[‡] These authors contributed equally to this work.

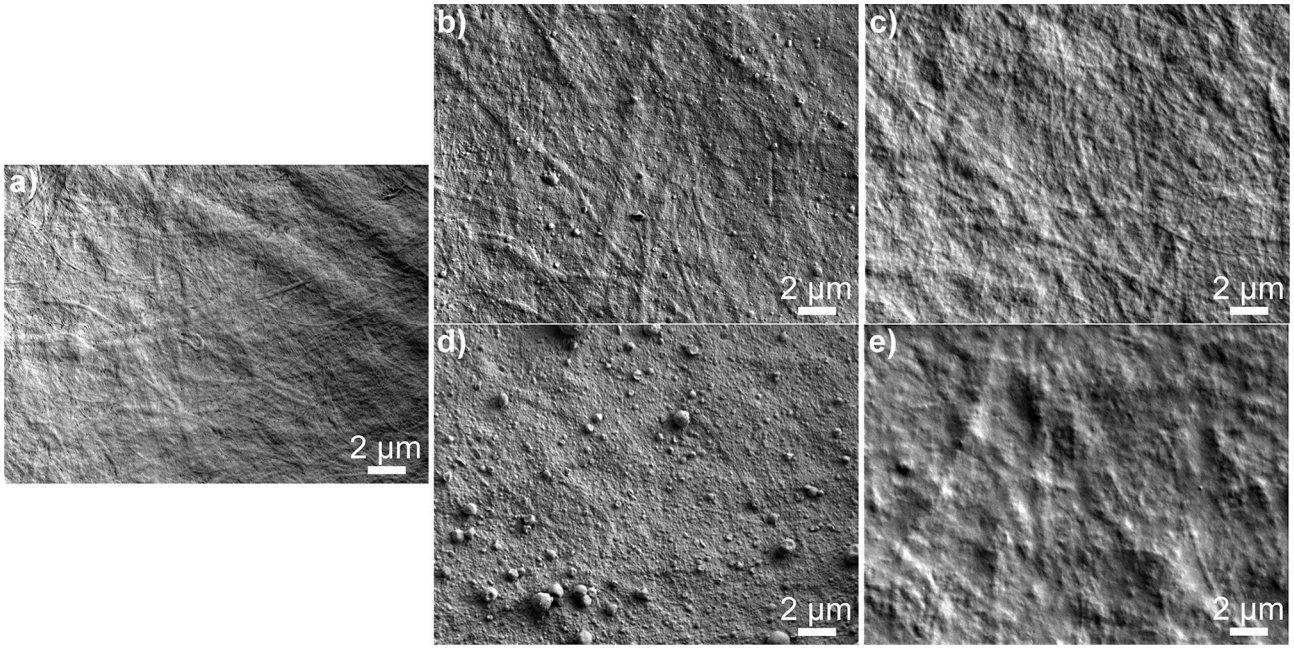

Fig. S1 The scanning electron microscopy (SEM) images of pure CNF film (a), CNF coated with 1BL of PLL/wax before (b) and after (c) thermal annealing, and CNF coated with 2BL before (d) and after (e) thermal annealing.

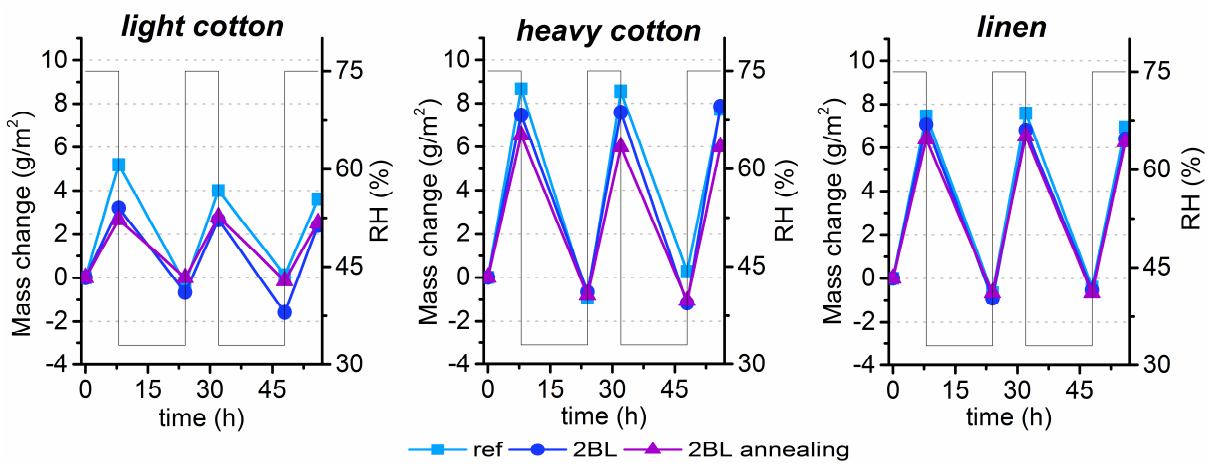

Fig. S2 Relative moisture uptake and release of uncoated and coated textiles. The lines on the graph connect measuring points and do not correctly illustrate the rate of change. The black line shows the relative humidity in the chamber.

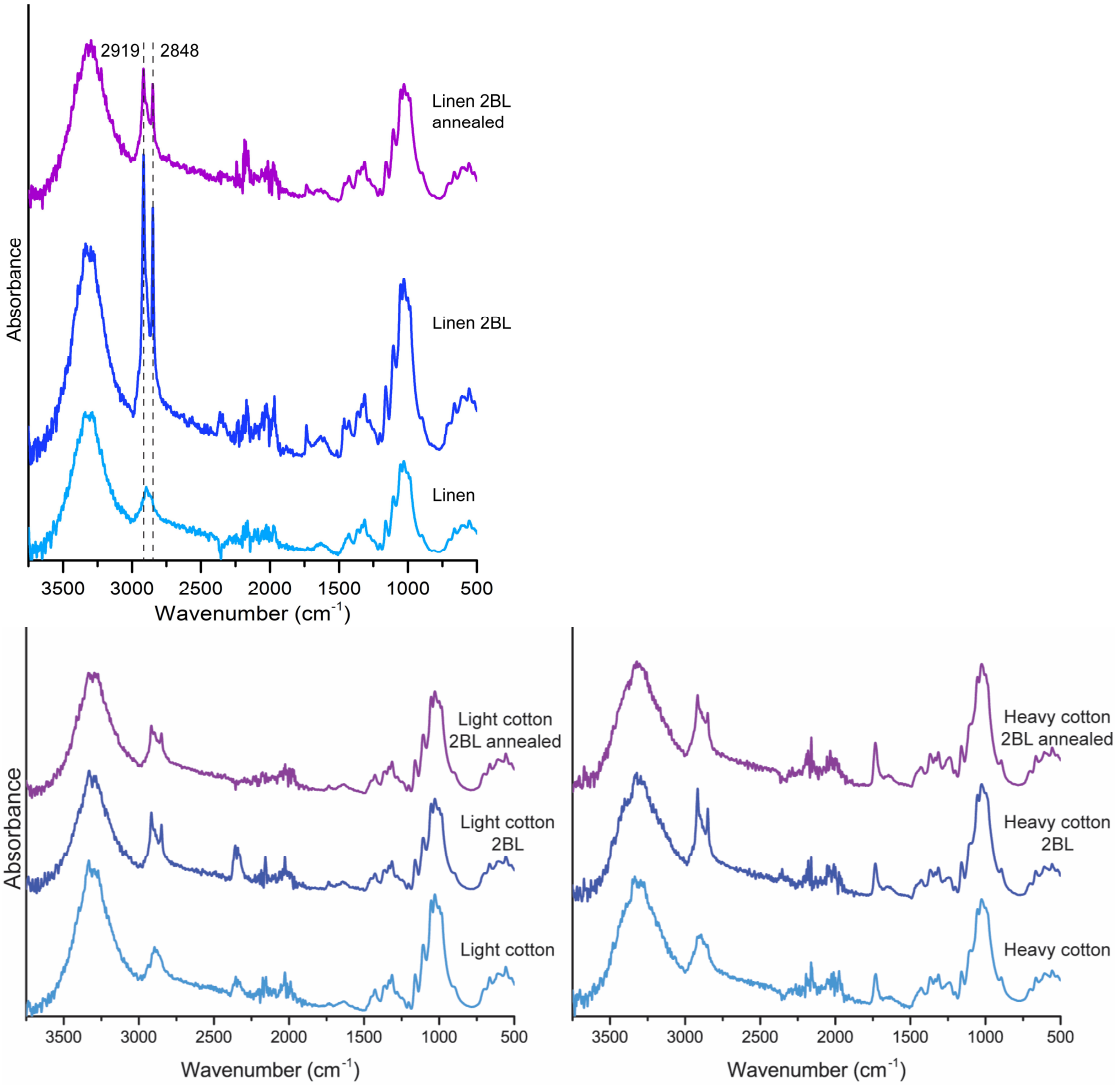

Fig. S3 FTIR spectra of untreated, coated with 2BL, and coated and annealed linen, heavy cotton and light cotton. The band at 1159 cm^{-1}, the C-O-C bridge, was used for normalization.

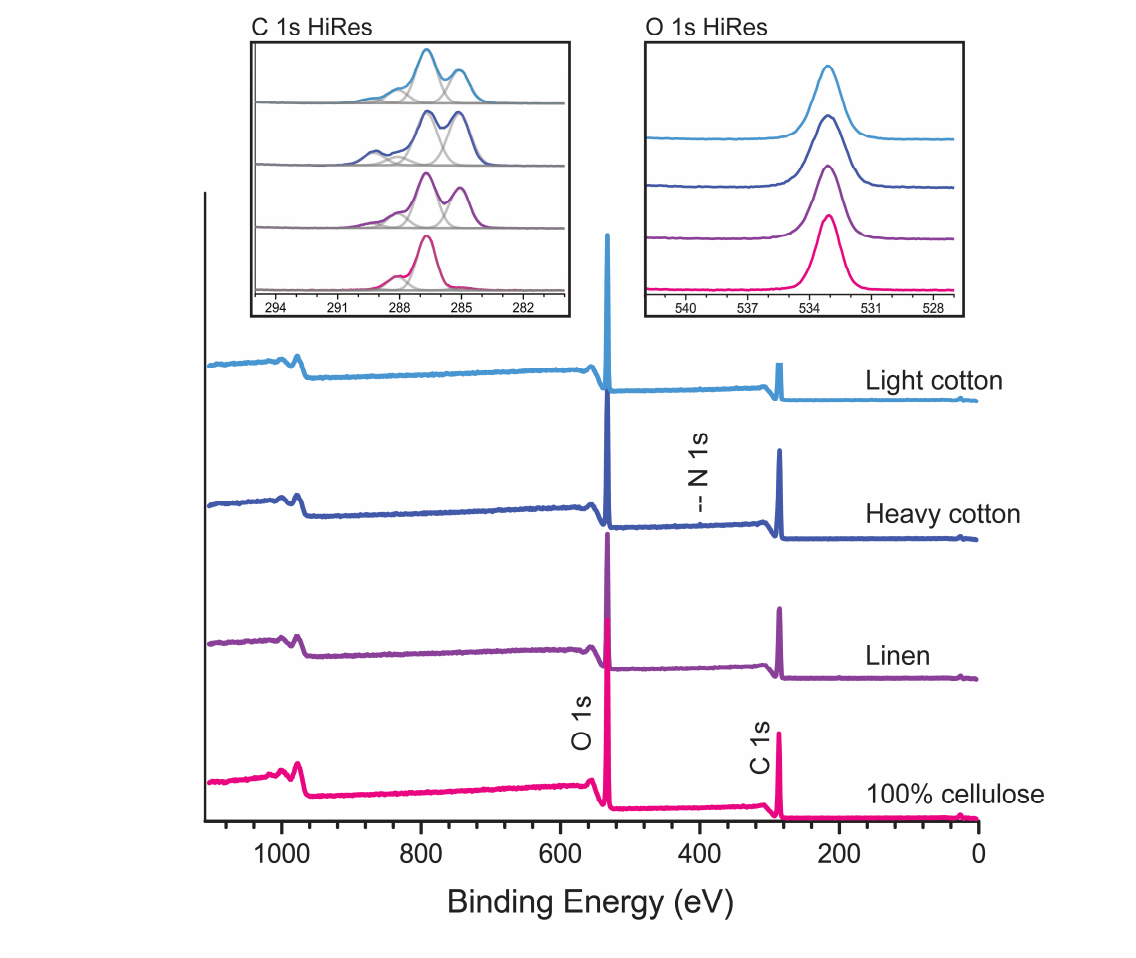

Fig. S4. XPS survey scans and high resolution XPS spectra of C 1s and O 1s regions of untreated light cotton, heavy cotton and linen as well as a pure cellulose used as a reference.

Vid1_Tilted cotton.mp4

Video S1. Water droplets on tilted uncoated and coated light cotton.

Vid2_Flat lying cotton.mp4

Video S2. Water droplets on flat lying uncoated and coated light cotton.